Title

CROSSED MOLECULAR BEAM STUDIES OF THE REACTIONS OF METHYL RADICALS WITH IODOALKANES

Authors

Robinson, G.N.
Nathanson, G.M.
Continetti, R.E.

Publication Date

1988-07-01

LBL-25553
Preprint

Lawrence Berkeley Laboratory
UNIVERSITY OF CALIFORNIA

Materials & Chemical Sciences Division

Submitted to Journal of Chemical Physics

Crossed Molecular Beam Studies of the Reactions of Methyl Radicals with Iodoalkanes

G.N. Robinson, G.M. Nathanson, R.E. Continetti, and
Y.T. Lee

July 1988

Prepared for the U.S. Department of Energy under Contract Number DE-AC03-76SF00098.

DISCLAIMER

Crossed Molecular Beam Studies of the Reactions of Methyl Radicals with Iodoalkanes

Gary N. Robinson[a], Gilbert M. Nathanson[b], Robert E. Continetti, and Yuan T. Lee

Materials and Chemical Sciences Division,
Lawrence Berkeley Laboratory and Department of Chemistry,
University of California, Berkeley, CA 94720

a) Present address: Department of Chemistry, Princeton University, Princeton, NJ 08544

b) Miller Research Fellow. Present address: Department of Chemistry, University of Wisconsin, Madison, WI 53706

ABSTRACT

The I atom exchange reactions, CH_3 + RI → CH_3I + R (R = CF_3, $(CH_3)_3C$), were investigated at a collision energy of ≈13 kcal/mol using the crossed molecular beams technique. The supersonic beam of methyl radicals was formed by pyrolyzing a mixture of ≈1% di-tert-butyl peroxide in helium in a quartz nozzle. A large fraction of the total energy available to the products from these reactions is channeled into relative translation (≈50% for R = $(CH_3)_3C$ and ≈70% for R = CF_3) suggesting that the dominant interaction among the products is repulsive. The CH_3I product from both reactions was observed to be entirely backward scattered with respect to the incident radical beam indicating that a roughly collinear C-I-C transition state geometry is favored. The present results are compared to those of earlier crossed beam studies of the CH_3 + IY → CH_3I + Y (Y = Cl, Br, I) reactions; the differences observed among these reactions are explained with reference to the CH_3I-Y and CH_3I-R interaction potentials.

I. INTRODUCTION

Free radical reactions are of central importance in atmospheric and combustion chemistry. Methyl radical abstraction reactions, in particular, play a key role in hydrocarbon fuel combustion. Although there have been numerous bulk gas-phase kinetic studies of such reactions (the majority of which have focused on H atom transfer [1]), very few free radical reactions of any sort have been investigated under single collision conditions.

Ross and co-workers [2,3] were among the first to use the crossed beams technique to study radical reactions. Using a tantalum oven to generate effusive beams of methyl and ethyl radicals, they investigated the halogen abstraction reactions $CH_3 + XY \rightarrow CH_3X + Y$, (XY = Cl_2, Br_2, I_2, ICl, and IBr) [2,3] and $C_2H_5 + Br_2 \rightarrow C_2H_5Br + Br$ [2b]. Grice and co-workers also studied the reactions $CH_3 + IY \rightarrow CH_3I + Y$ (Y = I, Br, and Cl) with an effusive radical source [4,5]. More recently they employed a supersonic CH_3 source to reinvestigate the IY and Br_2 reactions with improved velocity resolution [6].

In all of the crossed beam experiments, the RX product was observed to be predominantly backward scattered with respect to the incident radical beam. However, the CH_3I products from the IBr and ICl reactions were more sideways scattered than the CH_3X products from the homonuclear X_2 reactions. Product velocity measurements showed that the average fraction of available

energy going into product translation, $\langle E'/E_{avl} \rangle$, was ≈0.30 ± 0.05 for all of these reactions. However, the translational energy distributions for the IY reactions peaked at lower values of E' than those for the X_2 reactions. Somssich et al. [7] observed the CH_3Br product from the reaction $CH_3 + Br_2$ to be translationally hotter and more sideways scattered than Ross and co-workers [3]; they obtained $\langle E'/E_{avl} \rangle = 0.56$ whereas Ross reported a value of 0.26. Although these differences were attributed to the higher collision energy used in the experiments of Somssich et al., Grice's most recent work on $CH_3 + Br_2$ [6b], carried out at a comparable collision energy but with a supersonic radical beam, shows the CH_3Br product from this reaction to be strongly backward scattered with $\langle E'/E_{avl} \rangle = 0.33$.

The main conclusion from these studies was that the $CH_3 + X_2 \rightarrow CH_3X + X$ potential energy surfaces (PES) are largely repulsive in their exit valleys, channeling a significant fraction of the available energy into product translation; the $CH_3 + IY \rightarrow CH_3I + Y$ surfaces are apparently less repulsive. The results of these experiments strongly resembled those for the reactive scattering of D atoms with diatomic halogen molecules [8,9] suggesting that, at least as far as halogen atom exchange reactions are concerned, methyl radicals and hydrogen atoms behave quite similarly.

Using the crossed beams method, we began to investigate the reactions of methyl radicals with halogenated saturated and un-

saturated hydrocarbons in order to learn how the internal degrees of freedom of reactants and products are coupled to the reaction coordinate in radical abstraction and substitution reactions. In these studies, we used a pyrolysis source to generate a supersonic methyl radical beam. Unfortunately, we were unable to observe radical-for-atom substitution in any of the halogenated unsaturated systems that we studied, including those for which substitution was readily observed with Br [10] and Cl atoms [11]. This is due to the lower cross section for methyl radical (as compared to halogen atom) addition reactions which is related, in terms of reaction rate theory, to the lower Arrhenius A-factor and higher activation energy for such reactions (for $CH_3 + C_2H_4 \rightarrow C_3H_7$, log A = 8.5 and E_{act} = 7.7 kcal/mol whereas for $Cl + C_2H_4 \rightarrow C_2H_4Cl$, log A = 10.7 and E_{act} = 0 kcal/mol [12]).

We were, however, able to carry out studies of the I atom exchange reactions, $CH_3 + RI \rightarrow CH_3I + R$, where R = CF_3 and $C(CH_3)_3$ at 12 - 13 kcal/mol collision energies. The most striking result of these experiments is that the additional vibrational degrees of freedom of the molecular reagent appear to play a very limited role in product energy partitioning. In fact, the fraction of energy available to the products of these reactions that is channeled into translation is greater than that for the CH_3 + XY reactions described above, suggesting that the CH_3-I-R and CH_3-X-Y potential energy surfaces are rather different from one another.

The thermochemical data available for the $CH_3 + CX_3I \rightarrow CH_3I + CX_3$ (X = F, CH_3) reactions are still somewhat limited. Tomkinson and Pritchard [15] have measured $E_{act} = 7.5 \pm 1.0$ kcal/mol for $CH_3 + CF_3I \rightarrow CH_3I + CF_3$. Alcock and Whittle [16] obtained an activation energy of 3.3 ± 0.2 kcal/mol for the reverse reaction. If these measurements of the activation energies were reliable, they would imply that the forward reaction is endothermic by ≈4 kcal/mol. Earlier molecular beam photodissociation studies yielded $D_0^\circ(C-I) = 53.3 \pm 0.7$ [17] and 53.3 ± 0.2 [18] kcal/mol for CH_3I and $D_0^\circ(C-I) = 53.0 \pm 0.5$ kcal/mol [19] for CF_3I. According to these values, this reaction is essentially thermoneutral. However, recent high resolution molecular beam photodissociation experiments on CH_3I [20] give a more reliable value of $D_0^\circ(C-I) = 55 \pm 0.5$ kcal/mol, implying $\Delta H_0^\circ = -2$ kcal/mol.

Based on Benson's value of 51 kcal/mol for the C-I bond dissociation energy in $(CH_3)_3CI$ [13a] and the above values for $D_0^\circ(C-I)$ in CH_3I, $CH_3 + (CH_3)_3CI \rightarrow CH_3I + C(CH_3)_3$ should be exoergic by 2 - 4 kcal/mol.

II. EXPERIMENTAL

The crossed beam apparatus used in these experiments has been described elsewhere [21,22]. Two seeded, doubly differentially pumped beams were crossed at 90° in a collision chamber held at approximately 10^{-7} torr. The CH_3I product from both

reactions was detected at m/e=142 with a triply differentially pumped detector that rotates in the plane of the two beams.

The methyl radical beam was formed by bubbling ≈160 torr of helium through di-tert-butyl peroxide (DTBP, Pfaltz and Bauer) at -19°C (vapor pressure, v.p.≈2 torr) and expanding the mixture through a tapered quartz nozzle heated to ≈1000°C with a tantalum heater. The nozzle was fabricated by drawing a quartz tube (0.64 cm OD) to an inner diameter of ≈0.5 mm and then grinding the tip to an angle of 60°. The heating element consisted of a small square block (≈9 mm^2) of 1mm thick Ta spot-welded to a 0.5 mm thick strip of Ta. The Ta strip was attached to two bent molybdenum strips which were affixed to water cooled electrodes and served as springs. A 60° conical hole was drilled into the 1mm block to mate with the quartz nozzle which was painted with a colloidal graphite suspension. Fig. 1 is a drawing of the source. Typically, 120 A at 1.2 VAC were passed through the heater. A conical stainless steel skimmer with an orifice diameter of 1.5 mm was positioned ≈1.3 cm from the nozzle.

In order to minimize radical recombination, it was necessary to heat the quartz nozzle at the tip only. However, within a few hours of operating the source, a black polymeric deposit accumulated inside the nozzle that blocked the gas flow. By monitoring the source foreline pressure and the product signal at a reference angle, it was possible to determine when this clogging began to affect the experiment seriously. A thin drill bit (0.4 mm diameter) attached to a long piece of stainless

steel tubing and residing permanently in the gas feedline was used to unclog the nozzle in between experimental runs.

It was found that, over time, the Ta heater reduced the quartz nozzle to silicon. In addition, the beam gases oxidized the heater. As a result, the heating element and the quartz nozzle needed periodic replacement. After each replacement the velocity of the methyl radical beam was remeasured and adjusted to agree with the earlier value.

The CF_3I beam was formed by expanding 170 torr of a mixture of 12% CF_3I (SCM) in neon through a 0.15 mm diameter nozzle at 30°C. The $(CH_3)_3CI$ (Aldrich) beam was generated by bubbling 170 torr of neon through the reagent held at 0°C (v.p.≈20 torr). The mixture expanded through a 0.20 mm diameter nozzle warmed to 70°C. A conical stainless steel skimmer with an orifice diameter of 1.0 mm was positioned ≈0.9 cm from the nozzle for both beams. A second defining aperture was placed between the skimmer and the differential wall for the t-butyl iodide beam in order to reduce the background arising from impurities in the beam at detector angles close to 0°.

Product angular distributions were measured by modulating the methyl radical beam with a 150 Hz tuning fork chopper. Data were collected for approximately 12 minutes per angle. $\theta = -20°$ was used as a reference angle for subsequent time-normalization of the data for both reactions. No data was collected within 8° of the R-I beam.

The velocities of the reagent beams were measured using the

time-of-flight (TOF) technique. A multi-channel scaler [23] interfaced to an LSI 11/73 computer accumulated the data. The peak velocities (in units of 10^4 cm/s), v_{pk}, and speed-ratios, S [24], of the reagent beams were: CH_3: v_{pk}=27.0, S=7.0 (CF_3I experiment), v_{pk}=27.4, S=7.2 ($(CH_3)_3CI$ experiment); CF_3I: v_{pk}=6.0, S=12.5; $(CH_3)_3CI$: v_{pk}=7.0, S=10.6. The most probable collision energies, E_c, were 12.3 and 12.8 kcal/mol for the CF_3I and $(CH_3)_3CI$ reactions respectively. The spread in collision energy was ≈30% fwhm.

Since one molecule of DTBP decomposes into two methyl radicals and two acetone molecules, there was a significant contribution to the m/e=15 signal in methyl beam TOF from acetone cracking in the electron bombardment ionizer. Because of the spread in the electron energy of our ionizer, it was not possible to ionize the methyl radicals selectively by lowering the electron energy below the appearance potential for dissociative ionization of acetone (I.P.(CH_3) = 9.8 eV; A.P.($C_3H_6O \rightarrow CH_3^+ + CH_3CO + e^-$) = 13.2 eV [25]). In the early phase of this study, the presence of methyl radicals in the beam was determined by inspecting the width of the m/e=15 TOF peak. At low stagnation pressures, when the expansion from the nozzle was mild and slippage in the terminal velocities of different species was noticeable, one could observe a widening of the m/e=15 peak compared with those of heavier species in the beam. Upon increasing the stagnation pressure to achieve a more isentropic expansion, no widening was apparent and presumably the methyl

radicals and acetone molecules had the same terminal velocity distribution. All of the reactions were studied under such conditions.

Product TOF spectra were measured using the cross-correlation method [22]. A Cu-Be alloy disk photo-etched with a 255 channel pseudorandom sequence of open and closed slots was spun at 392 Hz giving 10 μs resolution in the TOF spectra. The resulting spectrum was deconvoluted by the on-line computer. The nominal flight-path from wheel to ionizer was 29.9 cm.

III. RESULTS AND ANALYSIS

A. $CH_3 + CF_3I \rightarrow CH_3I + CF_3$

The CH_3I (m/e=142) laboratory angular distribution for this reaction is shown in Fig. 2. The product is entirely backward scattered with respect to the incident CH_3 beam (the center-of-mass angle, θ_{CM}, is 19°). Elastic and inelastic scattering of impurities in the CF_3I beam by both He and acetone in the CH_3 beam contributed to a substantial modulated non-reactive m/e=142 signal at LAB angles from 0° to 15° and, to a lesser extent, from 0° to -5°. In order to subtract this background from the measured CH_3I angular distribution, we substituted a properly diluted beam of acetone in helium for the CH_3 beam produced from DTBP and measured the non-reactive scattering signal. The interpolated slope of the non-reactive scattering angular distribution from 8° to 20° was virtually identical to that

obtained with CH_3 radicals in the beam, suggesting that there is no reactive signal from CH_3 at 8°. In addition, the m/e=142 TOF spectrum at 8° did not change when acetone was substituted for DTBP. Since both the reactive and non-reactive angular distributions go to zero at 20°, this angle provides a rigorous upper limit to the width of the product angular distribution. Two possible experimental angular distributions are given in Fig. 2; one has N(8°)=0 and the other N(20°)=0.

In addition to the modulated background from in/elastic scattering, there was angle dependent unmodulated background at angles up to 12° from the CF_3I beam resulting from background molecules effusing from the differential region. The error bars for the points at -8° and -10° reflect the statistical noise associated with this unmodulated background.

Product TOF spectra were measured at three angles (Fig. 3). The signal-to-noise ratios are relatively low. The gradual drop in the CH_3 beam intensity caused by the decay of the heater and nozzle made it unprofitable to count for longer than about five hours at a given angle. Unmodulated background was subtracted from the TOF spectrum at -12° by measuring the m/e=142 TOF at this angle using beams of CH_3 in He and acetone in He. The -28° TOF spectrum has a long tail which is likely to be non-reactive in origin. The underlying shape of this tail is uncertain so it was not subtracted from the data.

The product angular distributions and TOF spectra were simultaneously fit using a forward convolution program [11] that

starts with a separable form for the center-of-mass (CM) reference frame product flux distribution,

$$I_{CM}(\theta,E') = T(\theta)P(E'),$$

and generates laboratory (LAB) frame angular distributions and TOF spectra suitably averaged over the spread in relative velocities. $T(\theta)$ is the CM frame product angular distribution. A three parameter functional form was used for P(E'), the CM frame product translational energy distribution:

$$P(E') = (E' - B)^p(E_{avl} - E')^q,$$

where B appears as a threshold in the distribution and is related to any barrier in the exit channel and $E_{avl}=(E_c-\Delta H^\circ_0)$. The calculated angular distributions and TOF spectra are scaled to agree with the experimental data.

We found that it was necessary to add ≈3 kcal/mol to the collision energy of 12.3 kcal/mol in order to fit the wide-angle part of the CH_3I angular distribution well. Thus, our data are in accord with an exoergicity of 2 kcal/mol. However, if the reaction is indeed thermoneutral, this could indicate that $v_{pk}(CH_3)$ is slightly higher than we infer from the peak m/e=15 flight time, t_{pk}. A decrease of 4 μsec in t_{pk} would increase $v_{pk}(CH_3)$ to 2.8×10^5 cm/s and raise the most-probable collision energy to 13.2 kcal/mol (the resolution was 1 μsec per channel for the beam TOF measurements). Some of this additional energy could also come from the out-of-plane vibrational mode (ν_2 = 606 cm^{-1} (1;0) and 681 cm^{-1} (2;1) [26]) of the methyl radical which is essentially directed along the reaction coor-

dinate. Assuming that the ν_2 mode is unrelaxed in the expansion, ≈50% of the methyl radicals will have at least one quantum in ν_2 and ≈40% will be in ν_2=1 at a nozzle temperature of 1000°C. It is worth noting that Brown et al. [5] were unable to fit their data for $CH_3 + ICl \rightarrow CH_3I + Cl$ without including part of the vibrational energy of the methyl radical in the total energy available. The spread in translational energy of their effusive radical beam is quite substantial, however, so it is unclear to what extent vibrationally excited methyl radicals were contributing to reaction.

Attempts were made to fit the data using differently shaped CM flux distributions. Both the N(8°)=0 and N(20°)=0 angular distributions could be fit with P(E') distributions having B values in the range 0 - 3 kcal/mol. The mean translational energy of the P(E') distributions (at the most-probable collision energy) increases from 9.9 - 10.2 kcal/mol on increasing B from 0 - 3 kcal/mol and adjusting p and q to optimize the fit. Thus, $\langle E'/E_{avl} \rangle \simeq 0.66$ over a range of B values. We present fits for B = 2 kcal/mol, p = 0.94, and q = 0.24 (Fig. 6a) in Figs. 2 and 3. With B = 2 kcal/mol, p can be decreased by as much as 30% (enhancing the low translational energy portion of the P(E') and lowering the peak energy by ≈1 kcal/mol) without significantly degrading the quality of the fits. Such a change amounts to a decrease of only 3% in $\langle E'/E_{avl} \rangle$.

A $T(\theta)$ distribution with T(65°)=0 (Fig. 7) has been used to fit the N(8°)=0 laboratory angular distribution and one with

T(90°)=0 was used for the N(20°)=0 fit. Since CH_3I product scattered backwards at angles up to ≈80° in the CM frame can contribute to the TOF spectra at all three LAB angles, the slow tails of the calculated TOF spectra are sensitive to the maximum angle of $T(\theta)$. However, because of the noise in the TOF data, both $T(\theta)$ distributions give acceptable fits to the spectra. Figs. 3 a,b show the fits generated using the two distributions.

Since the velocity spread of the CH_3 beam was not known exactly, we investigated the effect on the fits of decreasing the value of the CH_3 beam speed-ratio (equivalent to broadening the velocity spread). Decreasing S by 30% had a negligible effect on the calculated angular distribution. It did, however, broaden the calculated TOF spectra slightly, especially at -28° where it seemed to improve the fit. However, the poor signal-to-noise ratio at this angle makes it difficult to judge the quality of the fits.

Interestingly, we were unable to observe product from the reaction $CH_3 + CF_3Br \rightarrow CH_3Br + CF_3$ (ΔH°_{298} = 0 kcal/mol [27]) at a collision energy of 13 kcal/mol. This is presumably due to a higher potential energy barrier to this reaction. The activation energy for this reaction has been measured to be 12.5 kcal/mol [15].

B. $\underline{CH_3 + (CH_3)_3CI \rightarrow CH_3I + C(CH_3)_3}$

Elastic/inelastic scattering of impurities at m/e=142 was even more of a problem with $(CH_3)_3CI$ than with CF_3I. At 20°,

the modulated m/e=142 count rate was ≈40 Hz as compared to ≈15 Hz at -20°; the modulated m/e=142 count rate at 20° in the CF_3I experiment was essentially 0 Hz. As a result, it was not possible to subtract unambiguously the non-reactive contribution to the signal at $\theta > 0°$ for this reaction. Only data for $\theta \leq -8°$ are presented in Fig. 4 ($\theta_{CM} = 18°$). Again, substantial background signal from the unscattered $(CH_3)_3CI$ beam increased the statistical uncertainty at the angles closest to the beam. A TOF spectrum of CH_3I product at -20° is shown in Fig. 5 along with a m/e=142 TOF spectrum at -15° which includes both reactive and non-reactive components.

The small segment of the laboratory angular distribution that we obtained is from backward scattered products with relatively large recoil energies so the low recoil energy section of the P(E') cannot be definitively determined from the measured TOF spectra. The shape of the calculated TOF spectrum at -20° does not change on increasing the B parameter from 0-4 kcal/mol. A P(E') with B = 0 kcal/mol is used to obtain the fits presented in Figs. 4 and 5 (p = 1.02 and q = 0.92); we assume $\Delta H_0^\circ = -2$ kcal/mol. For this P(E'), $\langle E' \rangle = 7.6$ kcal/mol and $\langle E'/E_{avl} \rangle = 0.51$; $\langle E'/E_{avl} \rangle$ changes only slightly to 0.53 for the B = 3 distribution.

Acceptable fits to the m/e=142 angular distribution and TOF spectra are obtained with the T(90°)=0 and T(60°)=0 CM angular distributions shown in Fig. 7. The two fits are virtually identical for $\theta \leq -8°$. The calculated TOF spectra in Fig. 5a are

derived using the distribution that extends to θ=90°. The effect of truncating T(θ) at 60° is shown in Fig. 5b. The TOF spectrum at θ = -20° could not be fit well with a T(50°)=0 distribution. The noise in the TOF data again prevents us from being able to determine conclusively the length of the slow tail and hence the maximum angle of T(θ). Indeed, T(θ) could extend beyond 90°. Even with the uncertainty in T(θ), however, it is clear that the product is predominantly backward scattered.

IV. DISCUSSION

We have found that the CH_3I product from the CH_3 + RI reactions is strongly backward scattered with respect to the incident radical beam and that a large fraction of the total available energy appears in the relative motion of the recoiling products. $\langle E'/E_{avl} \rangle \simeq 0.66$ for R = CF_3 and $\approx$0.52 for R = $C(CH_3)_3$. These features are illustrated in Fig. 8 by the product flux contour diagram for $CH_3 + CF_3I \rightarrow CH_3I + CF_3$ in the CM reference frame.

As noted above, a threshold in the product translational energy distribution could result from a barrier in the exit channel of the reaction. Our best-fit P(E') distributions for $CH_3 + CF_3I \rightarrow CH_3I + CF_3$ are therefore consistent with the aforementioned kinetic study that suggests an activation energy

of ≈3 kcal/mol for the reverse reaction. Assuming that the reaction is thermoneutral and direct, the potential energy barrier in the forward direction will be of the same magnitude. The energy required to rehybridize the methyl carbon from sp^2 (radical) to sp^3 (CH_3I) may contribute to the barrier on the CH_3-I-CF_3 potential energy surface.

Although we have already noted the possibility that energy in the out-of-plane bend of CH_3 ends up in product translation, we cannot say if such energy helps to overcome the barrier to I atom exchange in the present reactions. There is no consensus in the literature on the effectiveness of the out-of-plane bend of CH_3 in promoting exchange reactions. Experiments by Ting and Weston [28] in which methyl radicals were generated by photolyzing CH_3Br suggest that energy in ν_2 can help to overcome the barrier to H atom transfer in the reaction $CH_3 + H_2 \rightarrow CH_4 + H$. Kovalenko and Leone [29] conclude from experiments with photolytically produced methyl radicals that reagent translational energy promotes the $CH_3 + Cl_2$ reaction but they were unable to assess the relative importance of translational energy against energy in the out-of-plane bend in driving the reaction. Finally, Chapman and Bunker [30] have found from trajectory calculations that depositing energy in ν_2 actually decreases the cross section for H atom transfer in $CH_3 + H_2$.

The large values of $\langle E'/E_{avl} \rangle$ obtained for the present reactions suggests that the dominant interaction between the CH_3I and CX_3 (X = F, CH_3) products beyond the transition state

is repulsive. If, in addition, the duration of the collision is short compared to the rotational period of the molecular reagent [31], one can correlate the angle at which the CM frame product angular distribution peaks with the energetically favored geometry of the reaction intermediate. Thus, the strong backward scattering that we observe indicates that a roughly collinear C-I-C transition state geometry is favored. Classical trajectory calculations on $D + I_2 \rightarrow DI + D$ [32] confirm the general validity of inferring the structure of the reaction intermediate from the product angular distribution for reactions on repulsive surfaces. However, trajectory calculations on $H + Br_2 \rightarrow HBr + H$ indicate that it is not always possible to correlate the anisotropy of the surface with the preferred scattering angle in a direct and simple manner [33].

It is instructive to compare our results for $CH_3 + CX_3I \rightarrow CH_3I + CX_3$ with those for $CH_3 + IY \rightarrow CH_3I + Y$, $D + IY$, and $D + CX_3I$ [34]. The CH_3I CM frame angular distributions obtained by Grice and co-workers [5,6b] range from ≈10°-180° for I_2 and from 0°-180° for ICl. Since the X groups will block sideways attack of the I atom, we might expect a narrower acceptance angle for the methyl radical and therefore enhanced backward scattering of CH_3I in the $CH_3 + CX_3I$ reactions. The narrow backward-peaked $T(\theta)$ distributions used to fit the CH_3I angular distributions for the present reactions are consistent with such a steric effect. Recent calculations by Benson indicate that the steric repulsion will be substantial when the C-I-C angle decreases

below 120^{o} [13b].

Our results for the CH_3 + CF_3I reaction are strikingly similar to those of Davidson et al. [35] for D + $CF_3I \rightarrow$ DI + CF_3 and of McDonald and Herschbach [36] for D + HI → DI + H. In both studies, the DI product was found to be entirely backward scattered with respect to the incident D atom beam, with $\langle E'/E_{avl} \rangle \approx 0.7$. This similarity recalls that between the CH_3 + IY and D + IY [8,9] crossed beam results. In studies of the D + IY → DI + Y reactions (Y = Cl, Br, and I) [8], the DI product was found to be predominantly sideways scattered with $\langle E'/E_{avl} \rangle =$ 0.24, 0.28, and 0.28 for Y = Cl, Br, and I respectively. Thus, the fraction of available energy in product translation for the (D, CH_3) + $CX_3I \rightarrow$ (D, CH_3)-I + CX_3 reactions is approximately twice the fraction that was observed for the IY reactions. Apparently, the (D, CH_3) + CX_3I potential energy surfaces are even more repulsive than those for (D, CH_3) + IY.

Although the degree of product repulsion in A + BC → AB + C reactions has been correlated with the location of the potential energy barrier along the reaction coordinate (i.e., the later the barrier, the stronger the repulsion) [37,38], classical trajectory calculations have shown that the slope of the potential energy surface along the retreat coordinate also affects the product energy distributions [39]. In addition, trajectory calculations indicate that as the collision energy is raised in an A + BC reaction, AB recoils from increasingly more compressed A-B-C intermediates, leading to enhanced product translation

[38,40]. This effect should be even more pronounced when A is considerably lighter than B and C since the AB bond will approach its equilibrium distance before the BC bond breaks [37,38]. Such "induced repulsive energy release" could be important in the present nearly thermoneutral reactions (where A = CH_3 and C = CX_3) for which the barrier is probably no more than a few kcal/mol.

In comparing values of $\langle E'/E_{avl} \rangle$ for the CH_3 + IY reactions, we note that the "attractiveness" of the CH_3-I-Y surfaces along the I-Y coordinate should increase with the electronegativity of the Y group [6b]. Work by Farrar and Lee [41] has shown that, at a collision energy of 2.6 kcal/mol, the reaction F + $CH_3I \rightarrow CH_3$ + IF proceeds through a long-lived collision complex that is bound by approximately 25 kcal/mol with respect to reactants and in which all of the vibrational degrees of freedom are equilibrated. Likewise, $O(^3P)$ and CF_3I form a long-lived CF_3-I-O complex at E_c=2.2 kcal/mol [42]. Although, by analogy with D-I-Cl [8,43], it is likely that CH_3-I-Cl is bent [4b], the CH_3 + ICl $\rightarrow$ CH_3I + Cl crossed beam results lead one to speculate that the CH_3-I-Cl surface has a shallow potential well that enables the intermediate to live long enough to rotate slightly and to undergo partial vibrational energy redistribution [3,5,6]. Recent work on Cl + $CH_3I \rightarrow CH_3$ + ICl [44] strongly suggests that a long-lived complex is formed at E_c=5.5 kcal/mol. The CH_3I angular distribution from CH_3 + IBr, E_c=7.6 kcal/mol [6] also shows substantial forward scattering.

It is therefore tempting to neglect the internal degrees of freedom of the CX_3 groups and to correlate the repulsive nature of the $CH_3 + CX_3I \rightarrow CH_3I + CX_3$ surfaces with the CX_3 electronegativities. Using the Mulliken method for calculating the electronegativity, χ, of an atom [45],

$$\chi = 1/2\ (IP + EA),$$

where IP is the ionization potential and EA is the electron affinity, we find that $\chi = 6.1$ eV for CF_3, below the value of 6.76 eV for I (see Table 1). $C(CH_3)_3^-$ has never been observed experimentally but kinetic measurements on the reaction of hydroxide ion with $(CH_3)_3SiC(CH_3)_3$ indicate that this anion is unbound by 0.3 eV [47]. Consequently, $\chi(C(CH_3)_3) \simeq 3.6$ eV [48]. By this crude measure, the CH_3-I-Y potential energy surfaces should be less attractive along the I-Y coordinate for Y = CX_3 than for Y = halogen atom.

Qualitative molecular orbital arguments indicate that the relative electronegativities of CH_3, I and Y correlate with important features of the CH_3-I-Y surfaces [4,8,49]. For iodine exchange through a collinear complex, the highest occupied molecular orbital is the σ^* orbital that is CH_3-I bonding and I-Y antibonding. This antibonding character leads to substantial repulsion between CH_3I and Y as the products separate. As Y becomes more electronegative, the σ^* and iodine p orbitals mix, leading to a bent transition state [50]. The I-Y antibonding interaction is reduced by this p orbital participation, lessening the repulsion between the products. Similar arguments

may apply to CH_3-I-CF_3 if the CF_3 group is treated as a single moiety. Although CF_3 is electron withdrawing, its electronegativity is lower than that of any halogen atom. In accord with the above discussion and the low electronegativity of CF_3, we observed both collinear reaction and sharp repulsive energy release for CH_3 + CF_3I. As mentioned earlier, these features will be further enhanced by the off-axis steric repulsion between both polyatomic species.

We still must answer the question of why the vibrational modes of the CX_3 fragments absorb so little energy during bond fission. The lack of vibrational excitation of the CF_3 fragment may be partly due to its having an equilibrium geometry that is almost identical to the geometry of the CF_3 group in CF_3I; the FCF bond angle in the radical is 111° [51] whereas in the molecule it is 108° [52]. Thus, there is no structural change to promote excitation of the out-of-plane bend which has a frequency of 701 cm^{-1} [51].

We must be careful in interpreting the modest difference in $\langle E'/E_{avl} \rangle$ between the two reactions, since we do not know how the potential energy surfaces differ. Let us assume, however, that the shape of the two surfaces along their reaction coordinates is the same. The simple fact that $C(CH_3)_3$ has more than four times the number of vibrational modes as CF_3 (neglecting the high frequency C-H stretching modes) can account for the greater amount of vibrational excitation of that fragment. The structure of $C(CH_3)_3$ has been the subject of considerable con-

troversy [48] but it appears to be slightly bent with a barrier to inversion of ≈0.5 kcal/mol [53,54]. Its ν_2 frequency has been estimated to be <200 cm^{-1} [55], more than three times lower than ν_2 in CF_3. Thus, excitation of ν_2 is more likely in $C(CH_3)_3$ than in CF_3.

Although C-I bond switching in the present reactions might not be as abrupt as C-I bond rupture in the photodissociation of iodoalkanes, we can use an impulsive model to calculate the fraction of energy expected in product translation in the "soft radical" limit. In this limit [56], repulsive C-I bond fission is considered to deliver an impulse to the carbon and iodine atoms only. The atoms are therefore treated as being independent of the groups to which they are bonded. Momentum is conserved between the C and I atoms; the momentum of each product is then taken to be equal to the momentum of its constituent recoiling atom. For both reactions, the translational energy of the product is considerably higher than what the "soft" impulsive model predicts: $\langle E/E_{avl} \rangle$ = 0.24 and 0.27 for CF_3I and $(CH_3)_3CI$ respectively whereas the experimental values are ≈0.7 and ≈0.5.

In the "rigid radical" limit, all of the available energy appears in product rotation and translation and, for a collinear reaction, solely in translation. However, even for non-collinear reactive geometries, the rotational energy of the products will be very small. For an impulsive CH_3 + CF_3I collision (E_c=12.3 kcal/mol, $\langle E' \rangle$ = 10 kcal/mol) with a C-I-C

angle of 150° at the critical configuration, the difference between the initial and final orbital angular momenta is only $\approx 15\ \hbar$. This amounts to less than 0.1 kcal/mol of rotational energy in CH_3I assuming no torque on the CF_3 fragment. Thus, our results fall somewhere in between the "soft" and "rigid" radical predictions.

It is worth comparing our reactive scattering results with data on the ultraviolet photofragmentation of iodoalkanes, where only one polyatomic product is internally excited. In these systems, C-I bond cleavage is believed to occur via excitation of a nonbonding $p\pi$ electron on the I atom to the σ^* antibonding C-I orbital [57]. Recent experiments by Zhu [58] on the photofragmentation dynamics of a series of iodoalkanes ($R\text{-}I \xrightarrow{248\ nm} R + I$) show that, on going from CH_3I to $(CH_3)_3CI$, the fraction of energy released into product translation decreases from 0.85 to 0.28. His value of $\langle E'/E_{avl} \rangle$ for $(CH_3)_3CI$ is in rough accord with the prediction of the "soft" impulsive model. In their work on the photodissociation of CF_3I [19] and CH_3I [18] at 248 nm, van Veen et al. found significantly greater vibrational excitation of CF_3 than CH_3 ($\langle E'/E_{avl} \rangle = 0.89$ for $CH_3I \rightarrow CH_3 + I^*$, 0.61 for $CF_3I \rightarrow CF_3 + I^*$) despite the large structural change that the CH_3 group undergoes upon C-I bond rupture. This difference was attributed to a steeper dissociative potential and a lower CX stretching frequency in CF_3I. Our value for $\langle E'/E_{avl} \rangle$ for $CH_3 + CF_3I \rightarrow CH_3I + CF_3$ agrees closely with the value for the $CF_3I + h\nu(248\ nm) \rightarrow CF_3 + I$, suggesting that the

repulsive interaction between during C-I bond fission in CF_3I might be similar in C-I bond switching and photodissociation. In the case of $(CH_3)_3CI$, however, the vibrational degrees of freedom of the t-butyl radical appear to be more efficiently excited during C-I photodissociation, though our reactive scattering data is limited here.

VI. CONCLUSIONS

We have presented the results of the first crossed molecular beam studies of the reactions of methyl radicals with polyatomic molecules. Our observations for the I atom exchange reactions, $CH_3 + CX_3I \rightarrow CH_3I + CX_3$ (X = F, CH_3), are remarkably similar to those of the analogous D atom reaction, $D + CF_3I \rightarrow DI + CF_3$, in that the CH_3I product is sharply backward scattered with most of the available energy going into product translation. The degree of product repulsion is greater than that observed for the reactions $CH_3 + IY \rightarrow CH_3I + Y$ (Y = Cl, Br, I). This can be rationalized in terms of differences in the stabilities of the reaction intermediates. The average fraction of energy released into product translation is ≈15% lower for $CH_3 + (CH_3)_3CI$ than for $CH_3 + CF_3I$. A higher probability of exciting the out-of-plane vibration of $C(CH_3)_3$ as compared to CF_3 is likely to be responsible for this decrease.

ACKNOWLEDGEMENTS

The electrode assembly for the methyl radical source was designed earlier in this laboratory by Dr. Timothy Minton. We thank Profs. Robert Squires and Frank Weinhold for helpful discussions. G. M. N. thanks the Miller Institute of the University of California for a fellowship. This work was supported by the Director, Office of Energy Research, Office of Basic Energy Sciences, Chemical Sciences Division of the U. S. Department of Energy under Contract No. DE-AC03-76SF00098.

REFERENCES

1. J. A. Kerr, in Comprehensive Chemical Kinetics, Vol. 18, "Selected Elementary Reactions", edited by C. H. Bamford and C. F. H. Tipper (Elsevier, Amsterdam, 1976), Ch. 2.
2. (a) D. L. McFadden, E. A. McCullough, Jr., F. Kalos, W. R. Gentry, and J. Ross, J. Chem. Phys. 57, 1351 (1972); (b) D. L. McFadden, E. A. McCullough, Jr., F. Kalos, and J. Ross, J. Chem. Phys. 59, 121 (1973).
3. J. A. Logan, C. A. Mims, G. W. Stewart, and J. Ross, J. Chem. Phys. 64, 1804 (1976).
4. (a) C. F. Carter, M. R. Levy, and R. Grice, Chem. Phys. Lett. 17, 414 (1972); (b) C. F. Carter, M. R. Levy, and R. Grice, Faraday Discuss. Chem. Soc. 55, 357 (1973).
5. L. C. Brown, J. C. Whitehead, and R. Grice, Mol. Phys. 31, 1069 (1976).
6. (a) S. M. A. Hoffman, D. J. Smith, J. H. Williams, and R. Grice, Chem. Phys. Lett. 113, 425 (1985); (b) S. M. A. Hoffman, D. J. Smith, N. Bradshaw, and R. Grice, Molec. Phys. 57, 1219 (1986).
7. P. Somssich, K. Strein and H. Schmiedel, Ber. Bunsenges. Phys. Chem. 85, 401 (1981).
8. J. D. McDonald, P. R. LeBreton, Y. T. Lee, and D. R. Herschbach, J. Chem. Phys. 56, 769 (1972).
9. J. Grosser and H. Haberland, Chem. Phys. 2, 342 (1973).
10. G. N. Robinson, R. E. Continetti, and Y. T. Lee, submitted

to J. Chem. Phys.

11. R. J. Buss, Ph. D. Thesis, University of California, Berkeley, 1979.

12. J. A. Kerr and M. J. Parsonage, Evaluated Kinetic Data on Gas Phase Addition Reactions (CRC, Cleveland, 1972).

13. a) S. W. Benson, Thermochemical Kinetics (Wiley, New York, 2nd ed., 1976); b) Acc. Chem. Res. 19, 335 (1986).

14. G. B. Ellison, P. C. Engelking, and W. C. Lineberger, J. Am. Chem. Soc. 100, 2556 (1978).

15. D. M. Tomkinson and H. O. Pritchard, J. Phys. Chem. 70, 1579 (1966).

16. W. G. Alcock and E. Whittle, Trans. Faraday Soc. 61, 244 (1965).

17. R. K. Sparks, K. Shobatake, L. R. Carlson, and Y. T. Lee, J. Chem. Phys. 75, 3838 (1981).

18. G. N. A. van Veen, T. Baller, A. E. de Vries, and N. J. A. van Veen, Chem. Phys. 87, 405 (1984).

19. G. N. A. van Veen, T. Baller, A. E. de Vries, and M. Shapiro, Chem. Phys. 93, 277 (1985).

20. Q. Zhu, E. J. Hintsa, X. Zhao, and Y. T. Lee (unpublished results); R. E. Continetti, B. A. Balko, and Y. T. Lee, submitted to J. Chem. Phys.

21. Y. T. Lee, J. D. McDonald, P. R. LeBreton, and D. R. Herschbach, Rev. Sci. Inst. 40, 1402 (1969).

22. R. K. Sparks, Ph. D. Thesis, University of California, Berkeley, 1979.

23. P. S. Weiss, Ph. D. Thesis, University of California, Berkeley, 1986.

24. R. B. Bernstein, Chemical Dyanmics via Molecular Beam and Laser Techniques (Oxford, New York, 198), p. 30.

25. J. L. Franklin, J. G. Dillard, H. M. Rosenstock, J. T. Herron, and K. Draxl, Ionization Potentials, Appearance Potentials, and Heats of Formation of Gaseous Positive Ions (NSRDS-NBS 26, US Dept. of Commerce, Washington, DC, 1969).

26. C. Yamada, E. Hirota, and K. Kawaguchi, J. Phys. Chem. 75, 5256 (1981).

27. CRC Handbook of Chemistry and Physics (CRC, Cleveland, 67th ed., 1986).

28. C. T. Ting and R. E. Weston, Jr., J. Phys. Chem. 77, 2257 (1973).

29. L. V. Kovalenko and S. R. Leone, J. Chem. Phys. 80, 3656 (1984).

30. S. Chapman and D. L. Bunker, J. Chem. Phys. 62, 2890 (1975).

31. For CH_3 + CF_3I, E_c=12.3 kcal/mol, the collision time is roughly 0.1 ps, assuming that the reagents interact over a range of 2Å. If we approximate CF_3I as a diatomic with a moment of inertia, I, of 331 amuÅ^2 (see ref. 52), its rotational distribution will peak at J=8 for a 10°K expansion, giving a rotational period, $2\pi I/J$, of ≈40 ps.

32. (a) J. D. McDonald, Faraday Discuss. Chem. Soc. 55, 372 (1973); (b) J. Chem. Phys. 60, 2040 (1974).

33. N. C. Blais and D. G. Truhlar, J. Chem. Phys. 61, 4186 (1974).

34. For D + IY → DI + Y, ΔH_0° = -35.8, -29.5, and -21.7 kcal/mol for Y=I, Br, and Cl respectively; for CH_3 + IY → CH_3I + Y, ΔH_0° = -19.4, -13.1, and -5.4 kcal/mol for Y=I, Br, and Cl respectively. D_0°(C-I) is taken to be 55 kcal/mol; values of D_0° for DI and IY were taken from, K. P. Huber and G. Herzberg, Molecular Spectra and Structure IV: Constants of Diatomic Molecules (Van Nostrand, New York, 1979).

35. F. E. Davidson, G. L. Duncan, and R. Grice, Mol. Phys. 44, 1119 (1981).

36. J. D. McDonald and D. R. Herschbach, J. Chem. Phys. 62, 4740 (1975).

37. P. J. Kuntz, E. M. Nemeth, J. C. Polanyi, S. D. Rosner, and C. E. Young, J. Chem. Phys. 44, 1168 (1966).

38. J. C. Polanyi and J. L. Schreiber, in Physical Chemistry: an Advanced Treatise, Vol 6A, "Kinetics of Gas Reactions", edited by W. Jost (Academic, New York, 1974), Ch. 6.

39. J. C. Polanyi and N. Sathyamurthy, Chem. Phys. 37, 259 (1979).

40. A. M. G. Ding, L. J. Kirsch, D. S. Perry, J. C. Polanyi, and J. L. Schreiber, Faraday Discuss. Chem. Soc. 55, 252 (1973).

41. J. M. Farrar and Y. T. Lee, J. Chem. Phys. 63, 3639 (1975).

42. R. J. Buss, S. J. Sibener, and Y. T. Lee, J. Phys. Chem. 87, 4840 (1983).

43. DIM calculations predict that HICl should be linear; I. Last and M. Baer, J. Chem. Phys. 80, 3246 (1984). However, ab initio calculations on H-I-F have shown that it has two minimum energy bent configurations- one with a bond angle of 82° another with an angle of 137°; R. J. Bartlett, L. Kahn and G. D. Purvis, J. Chem. Phys. 76, 731 (1982); R. J. Bartlett (private communication).

44. S. M. A. Hoffman, D. J. Smith, A. Gonzalez Ureña, and R. Grice, Chem. Phys. Lett. 107, 99 (1984); S. M. A. Hoffman, D. J. Smith, A. Gonzalez Ureña, T. A. Steele, and R. Grice, Mol. Phys. 53, 1067 (1984).

45. R. McWeeny, Coulson's Valence (Oxford University Press, Oxford, 3rd ed., 1979).

46. J. H. Richardson, L. M. Stephenson, and J. I. Brauman, Chem. Phys. Lett. 30, 17 (1975).

47. C. H. DePuy, V. M. Bierbaum, and R. Damrauer, J. Am. Chem. Soc. 106, 4051 (1984).

48. F. A. Houle and J. L. Beauchamp, J. Am. Chem. Soc. 101, 4067 (1979).

49. L. M. Lowenstein and J. G. Anderson, J. Phys. Chem. 91, 2993 (1987).

50. L. Pauling, The Nature of the Chemical Bond (Cornell Univ. Press, Ithaca, 1960).

51. C. Yamada and E. Hirota, J. Chem. Phys. 78, 1703 (1983).

52. C. H. Townes and A. L. Shawlow, Microwave Spectroscopy (Dover, New York, 1975).

53. D. Griller, K. U. Ingold, P. J. Krusic, and H. Fischer, J. Am. Chem. Soc. 100, 6750 (1978).

54. B. H. Lengsfield, III, P. E. M. Siegbahn, and B. Liu, J. Chem. Phys. 81, 710 (1984).

55. J. Pacansky, D. E. Horne, G. P. Gardini, and J. Bargon, J. Phys. Chem. 81, 2149 (1977).

56. K. E. Holdy, L. C. Klotz, and K. R. Wilson, J. Chem. Phys. 52, 4588 (1970).

57. R. S. Mulliken, Phys. Rev. 47, 413 (1935); J. Chem. Phys. 8, 382 (1940).

58. Q. Zhu, J. Cao, Y. Wen, J. Zhang, X. Zhong, Y. Huang, W. Fang and X. Wu, Chem. Phys. Lett. 144, 486 (1988).

Table 1. Mulliken electronegativities, χ, for atoms and radicals.

Atom/Radical	χ(eV)	Ref.
H	7.18	27
O	7.54	27
F	10.41	27
Cl	8.29	27
Br	7.59	27
I	6.76	27
CF_3	6.1	25,46
CH_3	4.96	27,48
$C(CH_3)_3$	3.6	47,48

FIGURE CAPTIONS

Fig. 1: Assembly drawing of methyl radical source. (1) tantalum block, (2) molybdenum springs; (3) water cooled copper electrodes; (4) precision ground quartz tube; (5) alumina spacers.

Fig. 2: CH_3I (m/e=142) product angular distribution for the reaction $CH_3 + CF_3I \rightarrow CH_3I + CF_3$. Center-of-mass angle is 19°. —— fit obtained with T(65°)=0 CM angular distribution in Fig. 6; — — fit obtained with T(90°)=0 distribution. Error bars represent 90% confidence limits. Radius of Newton circle in insert represents the maximum CM frame recoil velocity of the CH_3I product.

Fig. 3: CH_3I (m/e=142) time-of-flight spectra at three laboratory angles from the reaction $CH_3 + CF_3I \rightarrow CH_3I + CF_3$: (a) Solid line fit obtained with T(90°)=0 CM angular distribution in Fig. 7; (b) Solid line fit was obtained with T(65°)=0 CM angular distribution.

Fig. 4: CH_3I (m/e=142) product angular distribution for the reaction $CH_3 + (CH_3)_3CI \rightarrow CH_3I + (CH_3)_3C$. The fit was obtained with the T(90°)=0 CM angular distribution in Fig. 7. Error bars represent 90% confidence limits.

Fig. 5: CH_3I (m/e=142) time-of-flight spectra at two laboratory angles from the reaction $CH_3 + (CH_3)_3CI \rightarrow CH_3I + (CH_3)_3C$. (a) and (b) same as in Fig. 3. Non-reactive signal has not been subtracted from the $\theta = -15°$ spectrum.

Fig. 6: Center-of-mass frame product translational energy distributions: (a) Distribution used to fit $CH_3 + CF_3I$ data; (b) Distribution used to fit $CH_3 + (CH_3)_3CI$ data. See text for discussion of uncertainties in these distributions.

Fig. 7: Center-of-mass frame CH_3I angular distributions for both reactions. Dot dashed line = $T(60^o)$, solid line = $T(65^o)$, dashed line = $T(90^o)$.

Fig. 8: Center-of-mass flux contour diagram for the CH_3I product from $CH_3 + CF_3I \rightarrow CH_3I + CF_3$. The incident CH_3 and CF_3I velocity vectors have been truncated for clarity.

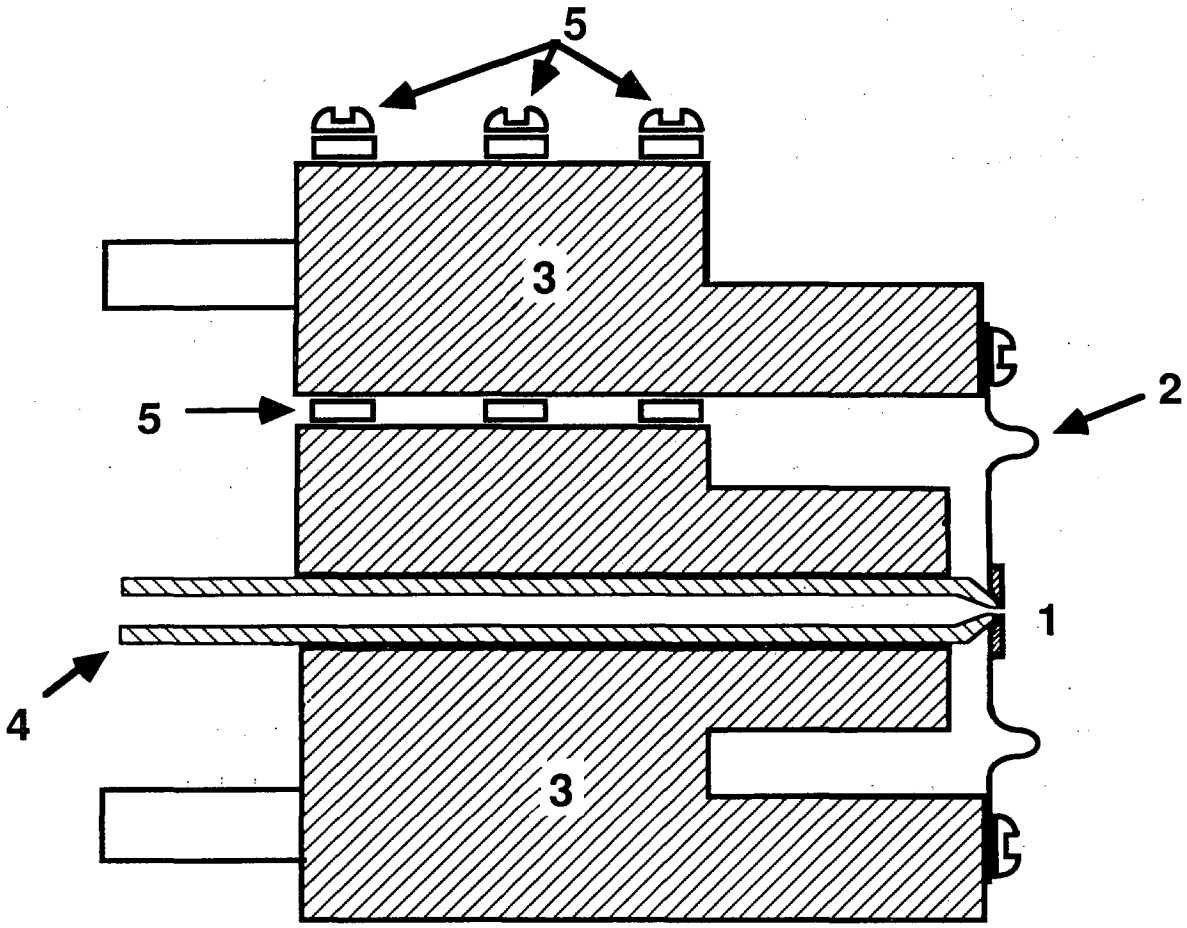

XBL 886-2155

Figure 1

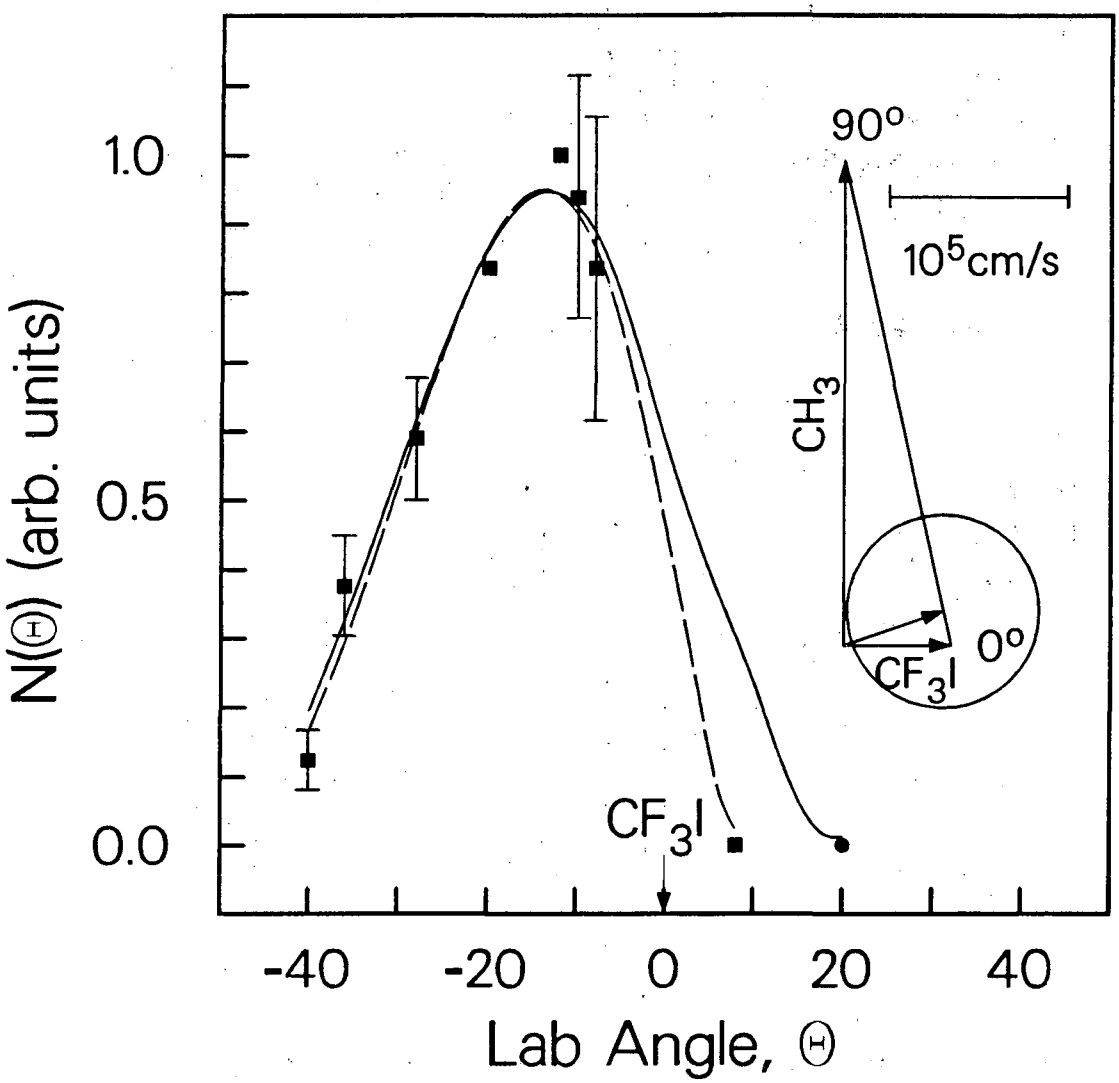

XBL 8712-5280A

Figure 2

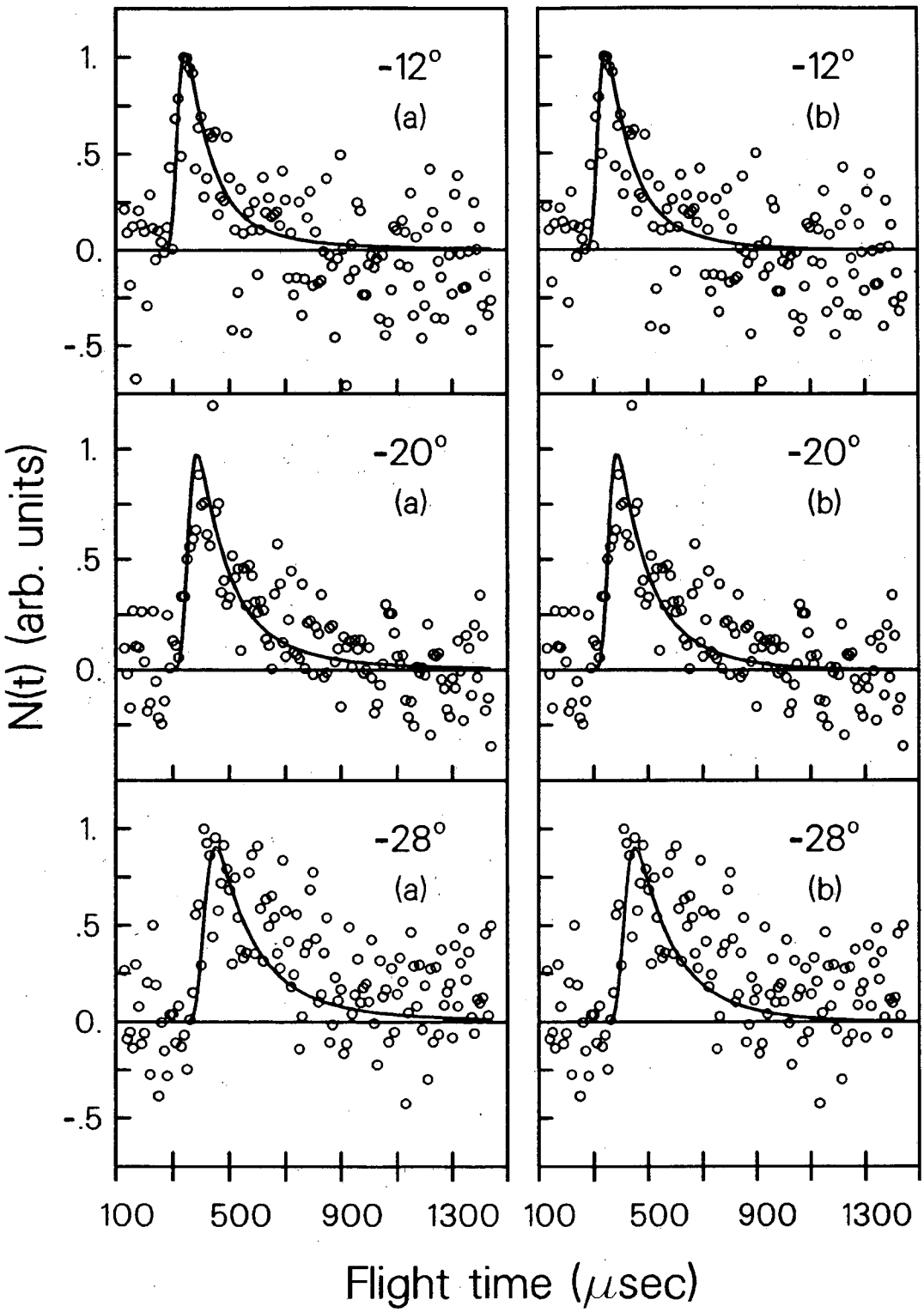

XBL 887-2377

Figure 3

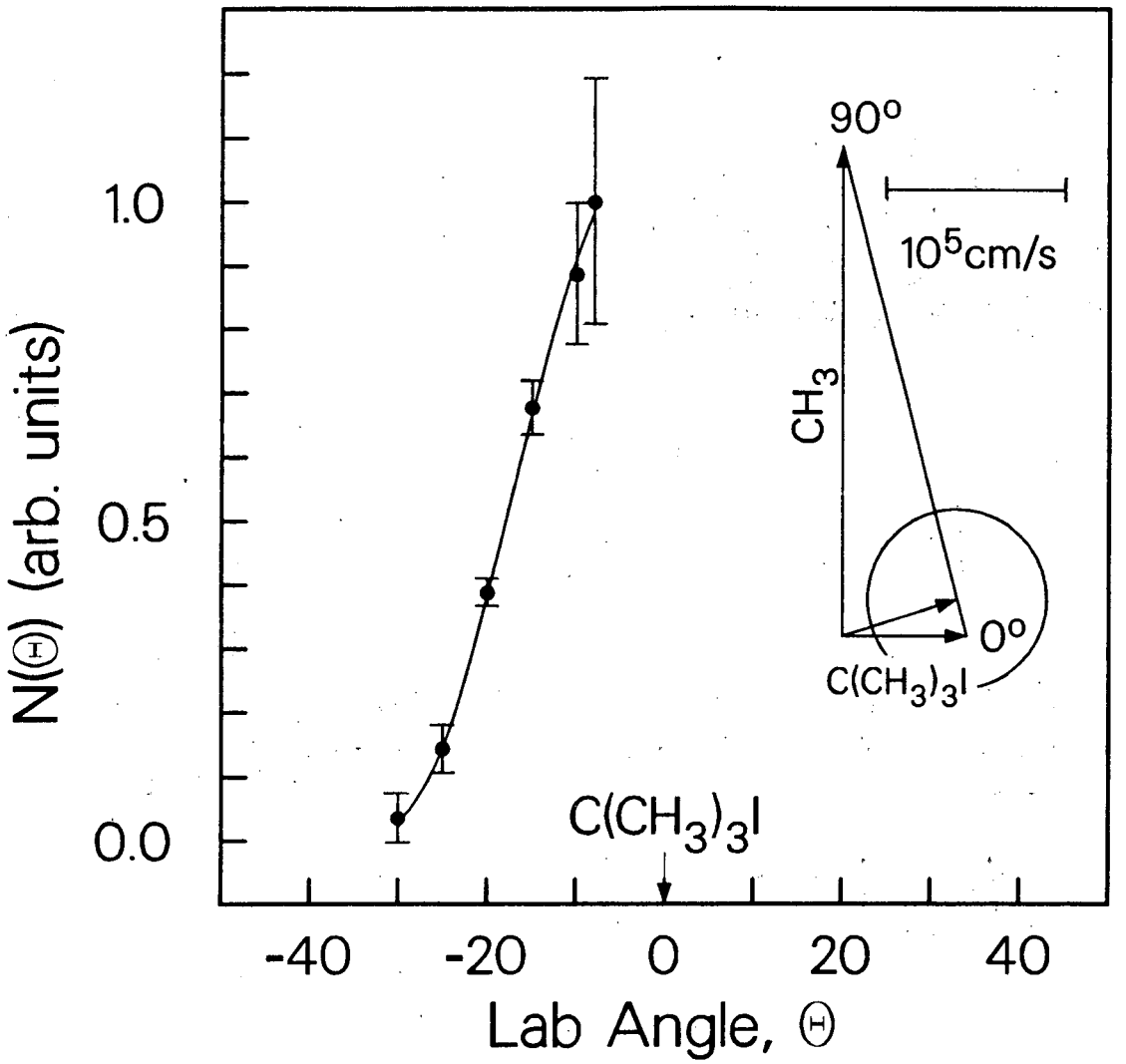

XBL 8712-5279A

Figure 4

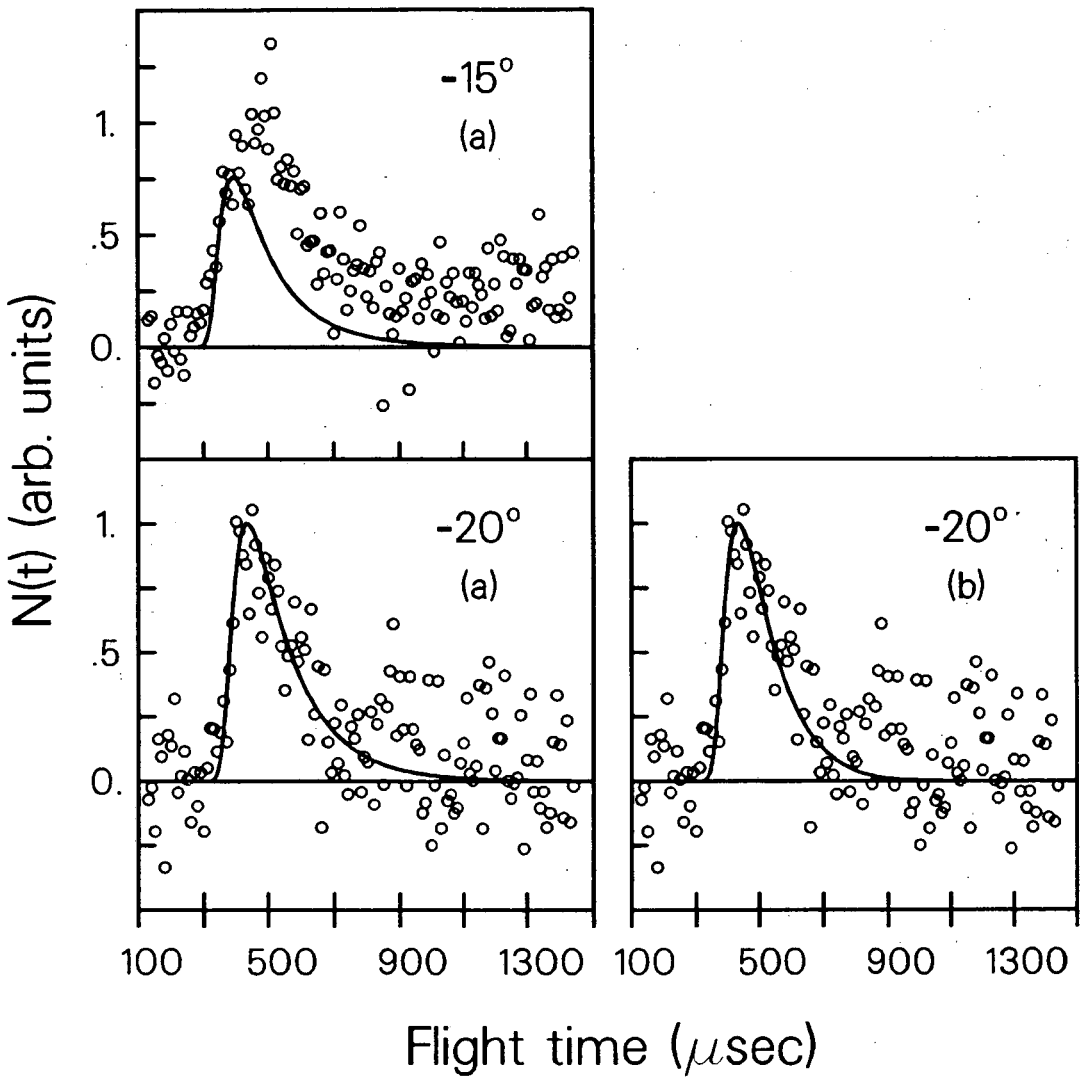

XBL 887-2378

Figure 5

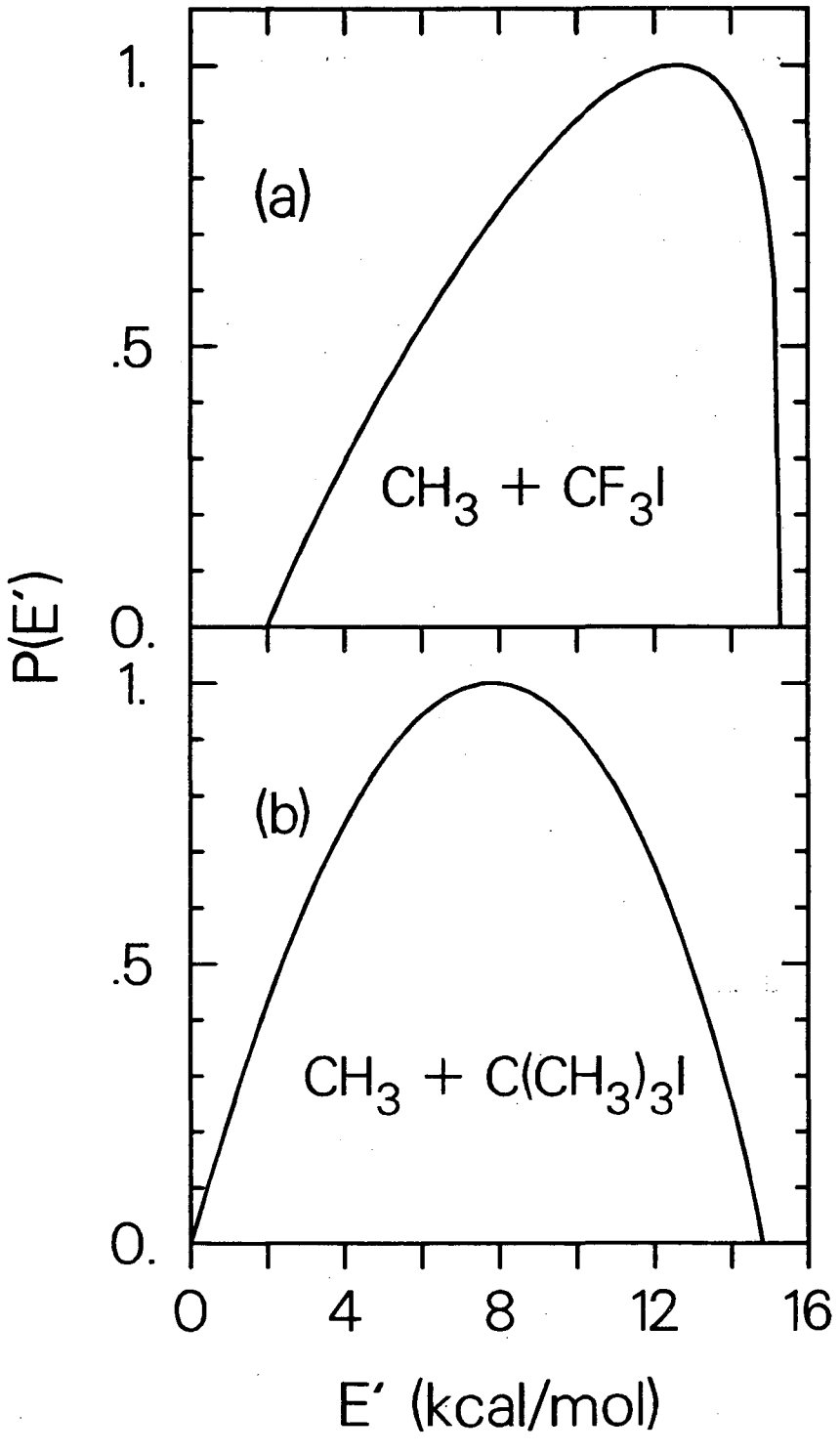

XBL 8712-5297A

Figure 6

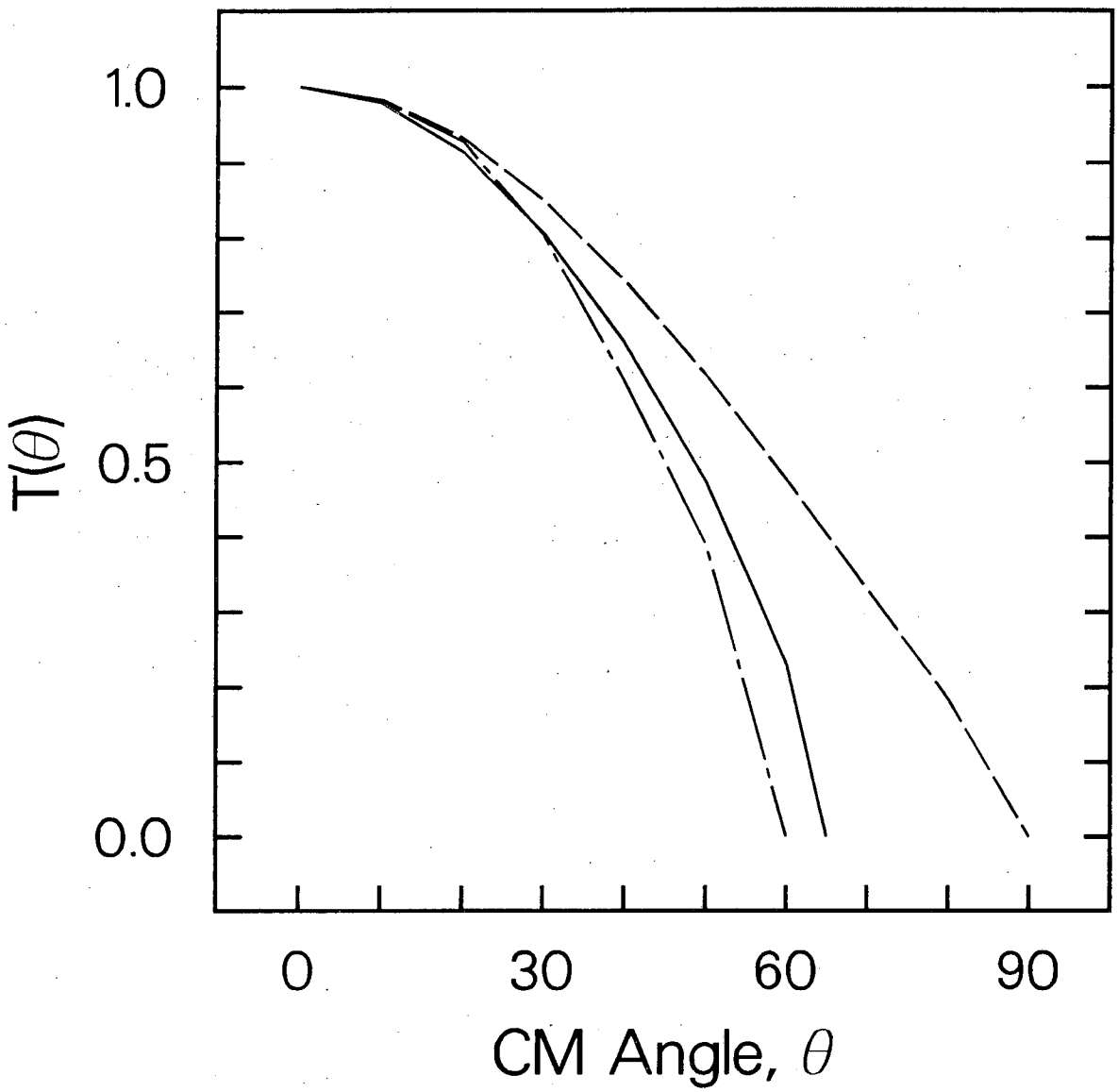

XBL 8712-5142A

Figure 7

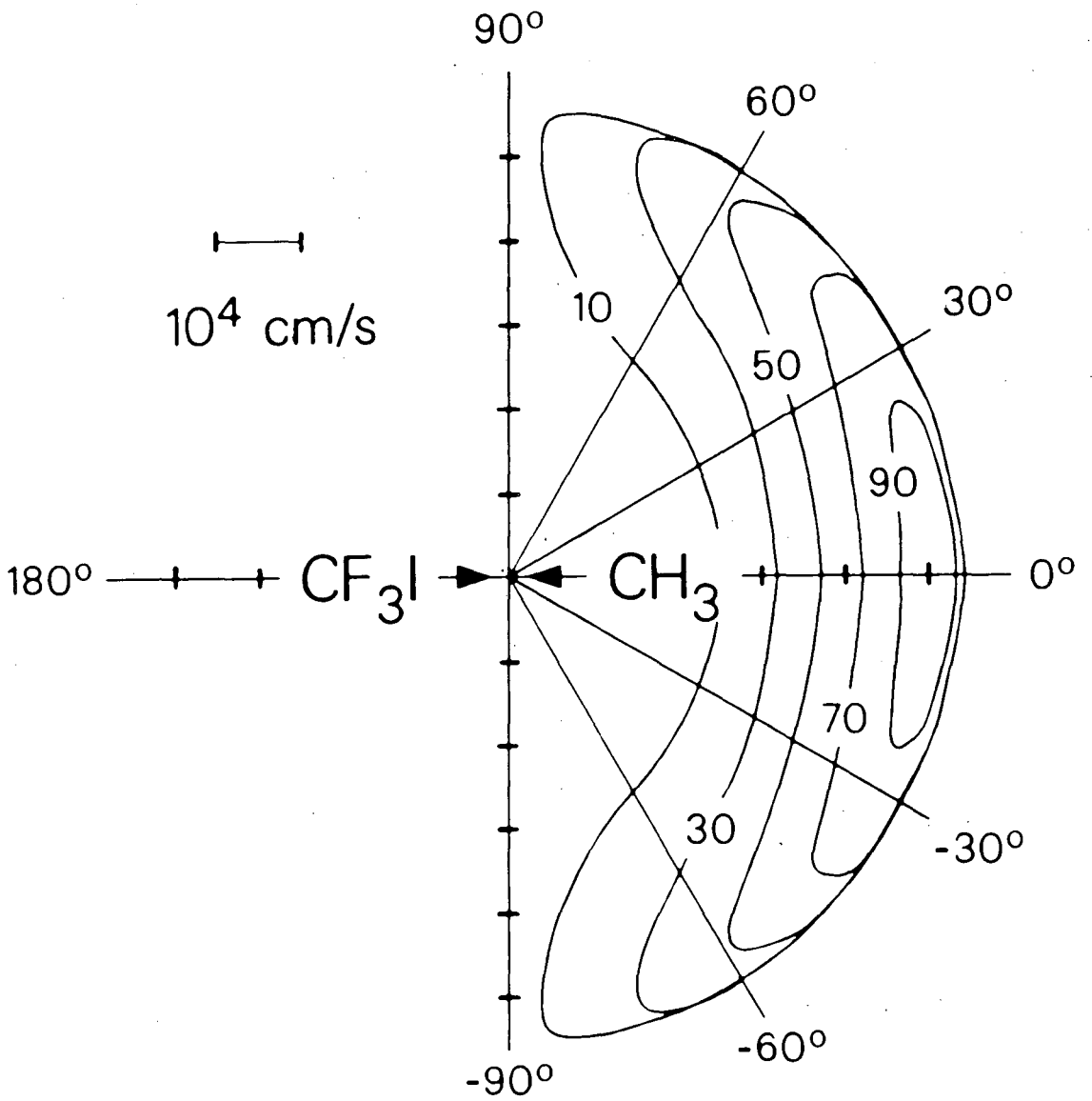

XBL 886-2078

Figure 8

LAWRENCE BERKELEY LABORATORY
TECHNICAL INFORMATION DEPARTMENT
UNIVERSITY OF CALIFORNIA
BERKELEY, CALIFORNIA 94720